Idealized neural responses

The mean firing rates (*fr*) of the idealized neurons shown in Fig. 4a–d, are given by equation (2) (from top to bottom, respectively):

$$fr = e^{-\left(\frac{T^2}{2}\right)}$$

$$fr = e^{-\left(\frac{T^2}{2} + \frac{H^2}{8}\right)} \qquad (2)$$

$$fr = e^{-\left(\frac{T^2}{4} + \frac{(T-H)^2}{4}\right)}$$

$$fr = e^{-\frac{(T-H)^2}{2}}$$

where T is the horizontal position of the target in eye coordinates, H is the horizontal position of the hand in eye coordinates, and $T - H$ is the horizontal position of the target in hand coordinates (see Fig. 1a). Our observations regarding these responses appear to be insensitive to both the form of these functions (gaussian versus sigmoid) as well as the nature of their interaction (multiplicative versus additive).

Gradient analysis

We estimated gradients from the data using an approximate numerical method (Matlab; Mathworks). The gradient resultant is a measure of the 'orientation' of an individual response field, and hence is an indicator of the variable or variables to which a neuron is most responsive (target position, initial hand position, and so on), regardless of the form of tuning (gaussian, sigmoid, and so on). To account for symmetrically shaped response fields we doubled the angles of the gradient vectors, then subtracted 360° from those angles greater than or equal to 360°, before taking the resultant[28]. This procedure transformed the data in such a way that resultants could be expressed easily in terms of their dependence on target position and initial hand position, as well as their sum and difference (Fig. 5c, e). Resultants could not, however, be mapped directly onto the response fields from which they were derived. For example, although neurons coding target position purely in hand-centred coordinates have obliquely oriented response fields (Fig. 4d), as points along the unity line correspond to identical hand-centred target positions, their gradient resultants would be expected to point straight down in Fig. 5c, e. Single cell and population resultants were normalized to unit length before plotting in Fig. 5.

Received 3 September 2001; accepted 25 January 2002.

1. Rondot, P., Recondo, J. & de Ribadeau Dumas, J. Visuomotor ataxia. *Brain* **100,** 355–376 (1977).
2. Kalaska, J. F., Caminiti, R. & Georgopoulos, A. P. Cortical mechanisms related to the direction of two-dimensional arm movements—relations in parietal area 5 and comparison with motor cortex. *Exp. Brain Res.* **51,** 247–260 (1983).
3. Georgopoulos, A. P., Caminiti, R. & Kalaska, J. F. Static spatial effects in motor cortex and area 5: quantitative relations in a two-dimensional space. *Exp. Brain Res.* **4,** 446–454 (1984).
4. Kalaska, J. F., Cohen, D. A. D., Prud'homme, M. & Hyde, M. L. Parietal area 5 neuronal activity encodes movement kinematics, not movement dynamics. *Exp. Brain Res.* **80,** 351 (1990).
5. Lacquaniti, F., Guignon, E., Bianchi, L., Ferraina, S. & Caminiti, R. Representing spatial information for limb movement: role of area 5 in the monkey. *Cerebr. Cortex* **5,** 391–409 (1995).
6. Kalaska, J. F. & Crammond, D. J. Deciding not to go: neuronal correlates of response selection in a go/nogo task in primate premotor and parietal cortex. *Cerebr. Cortex* **5,** 410–428 (1995).
7. Scott, S. H., Sergio, L. H. & Kalaska, J. F. Reaching movements with similar hand paths but different arm orientations. II. Activity of individual cells in dorsal premotor cortex and parietal area 5. *J. Neurophysiol.* **78,** 2413–2426 (1997).
8. Graziano, M. S. A., Cooke, D. F. & Taylor, C. S. R. Coding the location of the arm by sight. *Science* **290,** 1782–1786 (2000).
9. Battaglia-Mayer, A. *et al.* Early coding of reaching in the parietooccipital cortex. *J. Neurophysiol.* **83,** 2374–2391 (2000).
10. Flanders, M., Tillery, S. I. H. & Soechting, J. F. Early stages in a sensorimotor transformation. *Behav. Brain Sci.* **15,** 309–320 (1992).
11. Henriques, D. Y. P., Klier, E. M., Smith, M. A., Lowy, D. & Crawford, J. D. Gaze-centered remapping of remembered visual space in an open-loop pointing task. *J. Neurosci.* **18,** 1583–1594 (1998).
12. McIntyre, J., Stratta, F. & Lacquaniti, F. Short-term memory for reaching to visual targets: psychophysical evidence for body-centered reference frames. *J. Neurosci.* **18,** 8423–8435 (1998).
13. Jordan, M. I. & Rumelhart, D. E. Forward models: supervised learning with a distal teacher. *Cognitive Sci.* **16,** 307–354 (1992).
14. Batista, A. P., Buneo, C. A., Snyder, L. H. & Andersen, R. A. Reach plans in eye-centered coordinates. *Science* **285,** 257–260 (1999).
15. Strick, P. L. & Kim, C. C. Input to primate motor cortex from posterior parietal cortex (area 5). I. Demonstration by retrograde transport. *Brain Res.* **157,** 325–330 (1978).
16. Wiesendanger, R., Wiesendanger, M. & Ruegg, D. G. An anatomical investigation of the corticopontine projection in the primate (*Macaca fascicularis* and *Saimiri sciureus*). II. The projection from the frontal and parietal areas. *Neuroscience* **4,** 747–765 (1979).
17. Petrides, M. & Pandya, D. N. Projections to the frontal cortex from the posterior parietal region in the rhesus monkey. *J. Comp. Neurol.* **228,** 105–116 (1984).
18. Carozza, M., McIntyre, J., Zago, M. & Lacquaniti, F. Viewer-centered and body-centered frames of reference in direct visuomotor transformations. *Exp. Brain Res.* **129,** 201–210 (1999).
19. Andersen, R. A., Essick, G. K. & Siegel, R. M. Encoding of spatial location by posterior parietal neurons. *Science* **230,** 456–458 (1985).
20. Buneo, C. A., Batista, A. P. & Andersen, R. A. Frames of reference for reach-related activity in two parietal areas. *Soc. Neurosci. Abstr.* **24,** 262 (1998).
21. Desmurget, M. *et al.* Role of the posterior parietal cortex in updating reaching movements to a visual target. *Nature Neurosci.* **2,** 563–567 (1999).
22. Bullock, D., Cisek, P. & Grossberg, S. Cortical networks for control of voluntary arm movements under variable force conditions. *Cerebr. Cortex* **8,** 48–62 (1998).
23. Salinas, E. & Abbott, L. Transfer of coded information from sensory to motor networks. *J. Neurosci.* **15,** 6461–6474 (1995).
24. Deneve, S., Latham, P. E. & Pouget, A. Efficient computation and cue integration with noisy population codes. *Nature Neurosci.* **4,** 826–831 (2001).
25. Moran, D. W. & Schwartz, A. B. Motor cortical representation of speed and direction during reaching. *J. Neurophysiol.* **82,** 2676–2692 (1999).
26. Snyder, L. H., Batista, A. P. & Andersen, R. A. Coding of intention in the posterior parietal cortex. *Nature* **386,** 167–170 (1997).
27. Effron, B. & Tibshirani, R. J. *An Introduction to the Bootstrap* (Chapman & Hall, New York, 1993).
28. Zar, J. H. *Biostatistical Analysis* (Prentice-Hall, Upper Saddle River, New Jersey, 1999).
29. Andersen, R. A., Snyder, L. H., Li, C. S. & Stricanne, B. Coordinate transformations in the representation of spatial information. *Curr. Opin. Neurobiol.* **3,** 171–176 (1993).

Acknowledgements

This work was supported by the Defense Advanced Research Projects Agency (DARPA), the National Eye Institute, the Sloan-Schwartz Center for Theoretical Neurobiology, the James G. Boswell Foundation and an NIH training grant fellowship to C.A.B. We thank B. Gillikin and V. Shcherbatyuk for technical assistance; D. Dubowitz for collecting and processing the MRI data; J. Baer and J. Wynne for veterinary care; and C. Reyes-Marks for administrative assistance. We also thank J. Boline and K. Shenoy for comments.

Competing interests statement

The authors declare that they have no competing financial interests.

Correspondence and requests for materials should be addressed to R.A.A. (e-mail: andersen@vis.caltech.edu).

Chondroitinase ABC promotes functional recovery after spinal cord injury

Elizabeth J. Bradbury*, Lawrence D. F. Moon†§, Reena J. Popat*, Von R. King‡, Gavin S. Bennett*, Preena N. Patel*, James W. Fawcett† & Stephen B. McMahon*

** Sensory Function Group, Centre for Neuroscience Research, Hodgkin Building, Kings College London, Guy's Campus, London Bridge, London SE1 1UL, UK*
† Department of Physiology and Centre for Brain Repair, University of Cambridge, Robinson Way, Cambridge CB2 2PY, UK
‡ Department of Neuroscience, St Bartholomew's and the Royal London School of Medicine and Dentistry, Queen Mary, University of London, Mile End Road, London E1 4NS, UK

The inability of axons to regenerate after a spinal cord injury in the adult mammalian central nervous system (CNS) can lead to permanent paralysis. At sites of CNS injury, a glial scar develops, containing extracellular matrix molecules including chondroitin sulphate proteoglycans (CSPGs)[1,2]. CSPGs are inhibitory to axon growth *in vitro*[3–5], and regenerating axons stop at CSPG-rich regions *in vivo*[6]. Removing CSPG glycosaminoglycan (GAG) chains attenuates CSPG inhibitory activity[7–10]. To test the functional effects of degrading chondroitin sulphate (CS)-GAG after spinal cord injury, we delivered chondroitinase ABC (ChABC) to the lesioned dorsal columns of adult rats. We show that intrathecal treatment with ChABC degraded CS-GAG at the injury site, upregulated a regeneration-associated protein in injured neurons, and promoted regeneration of both ascending sensory projections and descending corticospinal tract axons. ChABC treatment also restored post-synaptic activity below the lesion after electrical stimulation of corticospinal neurons, and promoted functional recovery of locomotor and proprioceptive behaviours. Our results demonstrate that CSPGs are important

§ Present address: Miami Project to Cure Paralysis, 1095 NW 14th Terrace, PO Box 16960, Mail Locator R-48, Miami, Florida 33101, USA.

inhibitory molecules *in vivo* and suggest that their manipulation will be useful for treatment of human spinal injuries.

Adult rats received a cervical (C4) dorsal column crush lesion and bolus intrathecal infusions of protease-free ChABC or control solution. We assessed the degradation of CS-GAG at the injury site with the antibody 2B6, which recognizes an epitope on CSPG core proteins but not intact CS-GAG[10]. In control animals (unlesioned or lesioned and treated with vehicle) no 2B6 immunoreactivity was apparent (Fig. 1a). However, *in vitro* ChABC incubation of adjacent lesioned sections revealed extensive immunoreactivity (Fig. 1b), confirming the presence of CSPGs around the injury site. Lesioned rats treated *in vivo* with ChABC showed intense 2B6 immunoreactivity around the lesion site and in white matter tracts extending at least 4 mm rostrally and caudally (Fig. 1c, d). Thus, *in vivo* delivery of ChABC successfully removed GAG chains from CSPGs at and around the injury site.

Growth-associated protein 43 (GAP-43) is upregulated in primary sensory neurons after peripheral, but not central, nerve injury[11,12], and thus is associated with a regenerative state. We assessed GAP-43 expression after ChABC treatment in C5/6 dorsal root ganglia (DRG). In sham-operated controls, GAP-43 was present in 25% of small-diameter (less than 40 μm) and 6% of large-diameter (greater than 40 μm) neurons (Fig. 2a), and expression was similar in lesioned animals treated with vehicle (Fig. 2b). However, ChABC treatment increased GAP-43 in large-diameter cells (which project through the lesion site) to 22% ($P < 0.001$, analysis of variance (ANOVA), Fig. 2c). Thus, degrading GAG components of CSPGs promotes GAP-43 expression in injured neurons, indicating increased regenerative propensity in these cells.

Anatomical regeneration of injured dorsal column axons was assessed by labelling forelimb nerves with cholera toxin B-subunit (CTB). After lesion and infusion of vehicle, retraction of labelled fibres occurred, with few approaching, and none entering the lesion site (Fig. 2d). In contrast, in all lesioned animals that received ChABC infusions, thick fibre bundles approached the lesion (Fig. 2e). Notably, many axons traversed lesioned tissue, either

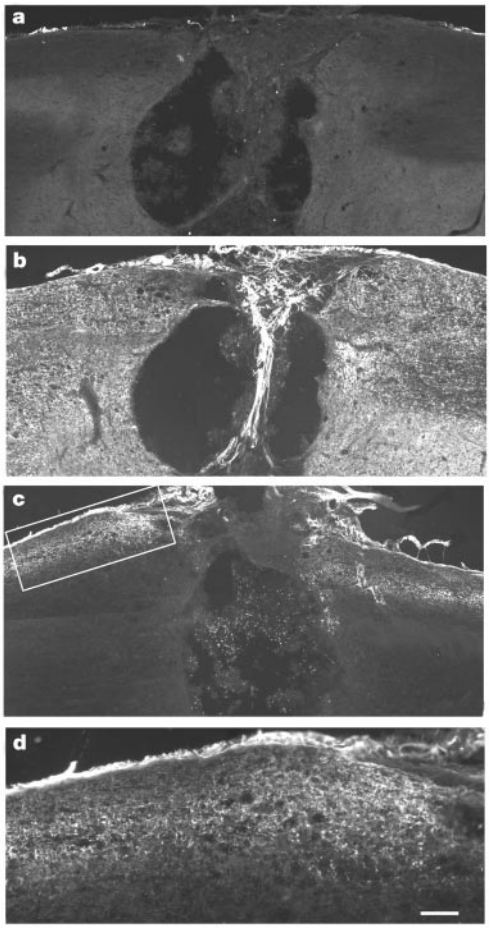

Figure 1 ChABC degrades CS-GAG *in vivo*. **a**, No 2B6 immunoreactivity is apparent in spinal cord sections after lesion and control infusions. **b**, Adjacent tissue incubated *in vitro* with ChABC shows intense immunoreactivity for 2B6 throughout the entire section, indicating an abundance of CSPGs in and around a site of spinal cord injury. **c**, After *in vivo* infusions of ChABC, 2B6 immunoreactivity is apparent at the lesion site and in the white matter, where spinal cord pathways project. **d**, High power of boxed area in **c**. Scale bar, 200 μm (**a**-**c**); 80 μm (**d**).

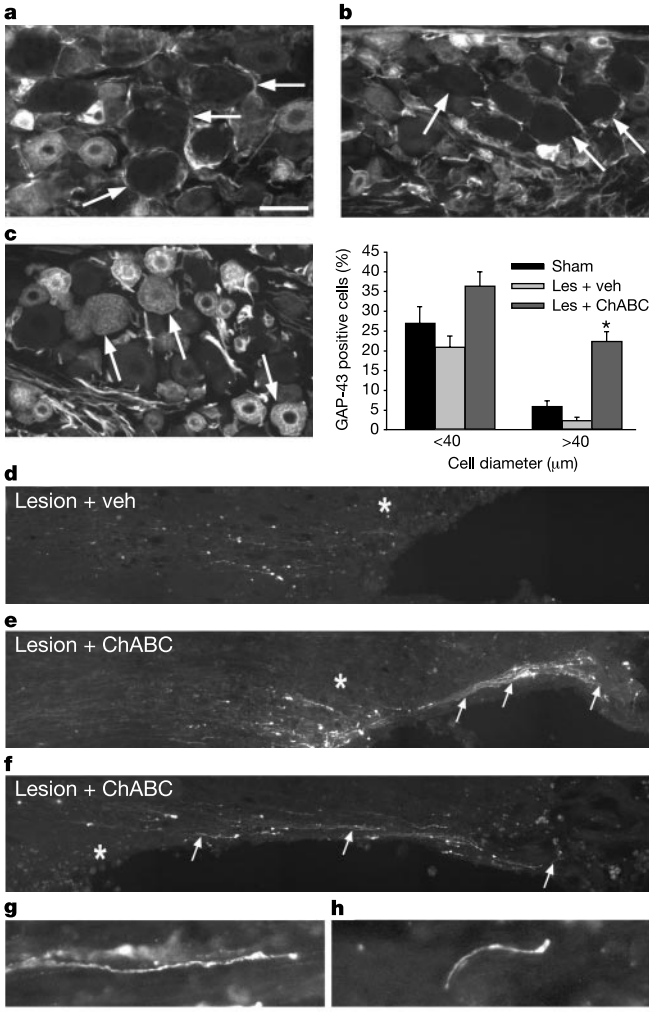

Figure 2 ChABC induces upregulation of GAP-43 in lesioned DRG neurons and regeneration of dorsal column axons. **a**, **b**, In control rats, GAP-43 protein expression is seen in a limited population of cervical DRG neurons (**a**), and does not change after lesion and control infusions (**b**; arrows in **a**, **b** indicate large-diameter neurons that do not express GAP-43). **c**, In contrast, a marked upregulation of GAP-43 expression is apparent after ChABC treatment, particularly in large-diameter DRG neurons (arrows). Quantification data (right) are means ± s.e.m. (asterisk denotes a significant difference from controls, $P < 0.001$, one-way ANOVA, Tukey post-hoc). Les, lesion; veh, vehicle. **d**, Axon tracing in the spinal cord reveals few CTB-labelled fibres proximal to the lesion after control infusions, with retraction bulbs indicating abortive regeneration. **e**, **f**, In contrast, after ChABC treatment many axons approach the lesion site and bundles of regenerating fibres traverse the lesioned tissue (arrows). **g**, **h**, Growth-cone-like endings are observed on regenerating fibres in lesioned animals treated with ChABC. Asterisks in **d**–**f**, indicate the lesion site. Scale bar, 50 μm (**a**–**c**); 400 μm (**d**–**f**); 20 μm (**g**, **h**).

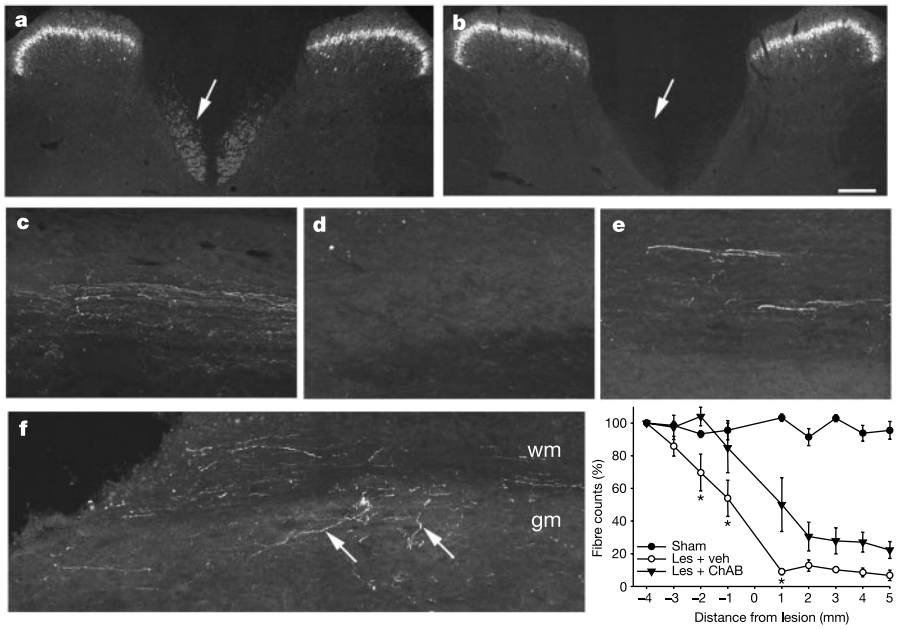

Figure 3 ChABC promotes regeneration of corticospinal tract axons. **a**, In control lumbar spinal cord, PKC-γ immunoreactivity is present in the dorsal horn and the CST. **b**, After a dorsal column lesion, PKC-γ immunoreactivity is no longer present in the CST (arrows in **a** and **b**), confirming a complete lesion. **c**, BDA-labelled CST fibres in the cervical spinal cord of controls. **d**, **e**, In lesioned animals BDA-labelled fibres are not observed below the injury site after vehicle infusions (**d**), but are present after ChABC infusions (**e**). **f**, In a ChABC-treated animal many axons are observed at the lesion site and appear to send collaterals (arrows) from white matter (wm) to grey matter (gm), indicating terminal arborization of regenerating axons. Quantification data (right) are percentages (means ± s.e.m.; asterisks denote significant difference between vehicle and ChABC treatment, $P < 0.05$, two-way ANOVA, Tukey post-hoc). Scale bar, 200 μm (**a**–**e**); 100 μm (**f**). Les, lesion; veh, vehicle.

growing around cavities or within the lesion epicentre (Fig. 2e, f). Growth-cone-like endings were apparent on axon tips in rats infused with ChABC (Fig. 2g, h), indicative of regeneration. Bundles of axons grew up to 2 mm through lesioned tissue, and many individual fibres were apparent 4 mm past the lesion site, indicating robust regeneration of dorsal column axons.

Regeneration of the major descending pathway in the dorsal columns, the corticospinal tract (CST), was also investigated. In unlesioned lumbar spinal cord, protein kinase C (PKC)-γ immunoreactivity (a marker of the CST[13]) was observed in the dorsal columns and lamina II (Fig. 3a). In all lesioned animals, no PKC-γ immunoreactivity was observed in the CST at lumbar levels (Fig. 3b), confirming complete transection of this tract. Regeneration of the CST was assessed using biotinylated dextran amine (BDA) injected into the motor cortex. In unlesioned animals, a thick fibre bundle was observed in cervical spinal cord (Fig. 3c). After dorsal column injury, CST axons had retracted from the lesion[14], and no fibres were seen beyond the lesion (Fig. 3d). However, ChABC treatment prevented CST retraction and promoted regeneration, with significantly more fibres seen at and below the lesion compared with vehicle treatment ($P < 0.001$, ANOVA, Fig. 3e). In ChABC-treated animals, some axons sent arborizing collaterals into grey matter (Fig. 3f).

Electrophysiological experiments determined that regenerated CST axons established functional connections. In anaesthetized control animals, electrical stimuli applied to motor cortex evoked large postsynaptic cord dorsum potentials (CDPs), as described previously[15], with an average latency of 3.9 ± 0.4 ms at C4 (Fig. 4). Acute dorsal column lesions largely abolished these CDPs below the lesion. The small remaining response presumably represents activation via non-dorsal column motor pathways. In vehicle-treated animals, CDPs were present above, but only minimally below the lesion ($P < 0.05$, ANOVA, Fig. 4). In contrast, ChABC-treated animals showed large CDPs up to 7 mm below the lesion, averaging about 40% of C3 CDP magnitude, significantly different from responses in vehicle-treated preparations ($P < 0.001$, ANOVA, Fig. 4). Responses had normal configurations, but were delayed (mean latency of 18.2 ± 2.6 ms, $P < 0.005$ compared with controls, *t*-test, Fig. 4), consistent with poor re-myelination of regenerating axons[16]. All ChABC-treated animals showed similar responses, which were abolished by acute dorsal column re-section; strong evidence of new connections of regenerated CST axons.

Dorsal column projections are important for discriminative touch and proprioception, and—together with local spinal reflexes—for skilled motor function. Rats were assessed by several behavioural tasks of forelimb function requiring sensorimotor skills. Adhesive tape-removal tasks assessed sensory (awareness of the tape) and motor (ability to remove the tape) function (Fig. 5a, b); unlesioned sham controls could perform these tasks quickly. Lesioned rats were severely impaired with or without ChABC treatment. These impairments persisted throughout six weeks of testing, consistent with the failure of ChABC treatment to promote regeneration to hindbrain sensory nuclei (6 weeks post-lesion latencies were: 7.4 ± 1.4 s and 3.8 ± 0.5 s (sham); 54.9 ± 3.1 s and 48.0 ± 4.4 s (lesion plus vehicle); 41.7 ± 8.3 s and 40.5 ± 11.1 s (lesion plus ChABC), for sense and removal tasks, respectively, $P < 0.001$, ANOVA, Fig. 5a, b). The number of forelimb foot slips were recorded when rats crossed a narrow beam or grid. In both tasks, unlesioned sham controls made few foot slips but vehicle-treated lesioned rats were severely and significantly impaired throughout testing, albeit with some recovery over time[17]($P < 0.001$, ANOVA; at 6 weeks after lesion, foot slips had increased compared with sham controls, from 0 ± 0 to 21.1 ± 4.2 and 0.8 ± 0.5 to 8.8 ± 1.9 on the beam and grid, respectively, Fig. 5c, d). ChABC treatment produced a marked recovery of function, with improvements from 2 weeks (beam) and 1 week (grid) onwards (not significantly different from sham controls, $P > 0.1$, ANOVA; at 6 weeks after lesion, foot slips were 2.6 ± 0.8 and 1.6 ± 0.7 on the beam and grid, respectively, Fig. 5c, d). Walking patterns were then assessed by analysing footprint spacing. Vehicle-treated lesioned rats took significantly shorter and wider strides than sham controls (stride length, 118.1 ± 6.3 mm versus

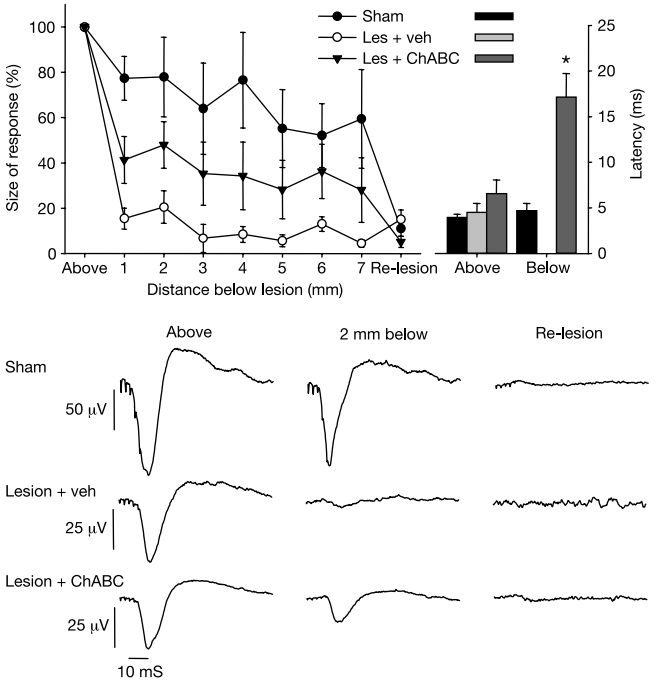

Figure 4 ChABC restores functional connections of descending motor pathways. Graph shows the average size of cortical evoked cord dorsum potentials (CDPs) 1 segment above C4 (lesion site) and at 1 mm intervals caudal to this site (data normalized to the size of the rostral recording). ChABC treatment increases CDPs below the lesion ($P < 0.001$, two-way ANOVA, compared with vehicle). Representative sample traces show that cortical stimulation normally evokes a short-latency negative–positive wave, which is absent 2 mm below an acute or chronic dorsal column lesion, but is partially restored by ChABC treatment. Notably, this restored activity is abolished by a re-lesion, indicating CST regeneration. The bar graph shows no differences in response latencies above the lesion ($P > 0.1$, one-way ANOVA) but below the lesion (measurement not possible in vehicle-treated preparations due to absence of evoked activity) latencies are longer in ChABC-treated animals (asterisk denotes significant difference from sham group, $P < 0.005$, *t*-test).

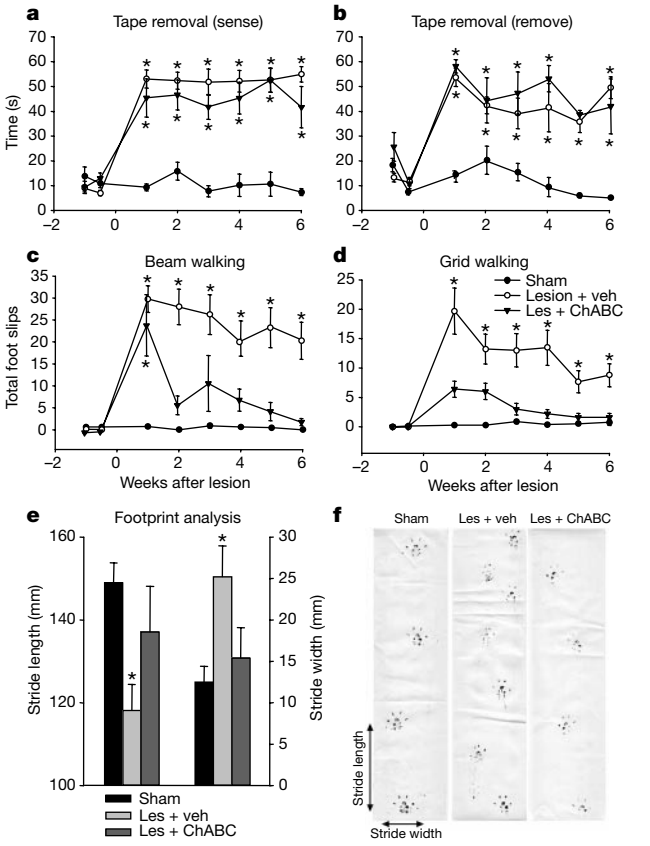

Figure 5 Functional recovery after ChABC treatment. **a**, **b**, In a tape removal task, lesioned rats treated with either vehicle solution or ChABC were severely impaired, compared with sham controls, both in their ability to sense and subsequently remove the adhesive tape. **c**, **d**, In the beam and grid tasks, lesioned rats treated with vehicle made significantly more foot-slip errors than controls. In contrast, lesioned rats treated with ChABC made a marked functional recovery on both these tasks. **e**, Footprint analysis revealed impaired walking patterns in lesioned rats treated with vehicle, with the strides becoming shorter and wider than controls; again, functional recovery was observed in lesioned rats treated with ChABC, with both the length and width of strides taken not significantly different from controls. **f**, Representative footprints from each group. Data are mean ± s.e.m. (asterisks denote significant difference from sham controls, $P < 0.02$, ANOVA, Tukey post-hoc).

148.9 ± 4.8 mm; width, 25.2 ± 3.7 mm versus 12.5 ± 1.9 mm; 6 weeks after lesion, $P < 0.02$, ANOVA, Fig. 5e, f). ChABC treatment largely prevented changes (length and width were 137.1 ± 11.0 mm and 15.4 ± 3.6 mm, respectively, not significantly different from shams, $P > 0.1$, ANOVA, Fig. 5e, f).

Our results demonstrate, using anatomical, electrophysiological and behavioural outcomes, that ChABC promotes regeneration and restores function after spinal cord injury. Several CSPGs, including neurocan, phosphacan and NG2, are upregulated at CNS injury sites[18–21], and we have shown that CS-GAG chains contribute towards regenerative failure. Anatomical regeneration was limited, presumably due to other inhibitory factors in lesioned spinal cord[22,23]. However, we observed very clear recovery of function after ChABC treatment, for which there are several possible anatomical substrates. First, a limited regrowth of sensory and CST motor axons might account, by means of new local segmental connections, for the behavioural recovery. Second, CSPGs may inhibit intact pathways from sprouting, allowing ChABC treatment to result in beneficial compensatory sprouting mechanisms, as reported for IN-1 treatment[24]. Chondroitinase ABC, and other potential treatments that affect CSPG production after injury, join blockade of NogoA, neurotrophic factor treatment, gene therapy and cellular grafting[25–28] as interventions that promote spinal cord regeneration, and may have therapeutic potential for the treatment of human spinal cord injuries. □

Methods

Spinal cord injury and ChABC treatment

Anaesthetized (sodium pentobarbital, 40 mg kg^{-1}) adult male Wistar rats received a bilateral lesion to the dorsal columns[29] at spinal level C4. Concurrently, a silastic tube was inserted intrathecally to lie just rostral to the lesion site, and externalized to deliver bolus injections of high-purity, protease-free chondroitinase ABC (ChABC; Seikagaku Corporation). Immediately after the lesion, 6 μl ChABC (10 U ml^{-1}) was injected followed by a 6-μl saline flush ($n = 17$). A further group received the spinal cord lesion with either saline or control enzyme treatment (Penicillinase, Sigma; same μg protein delivered, $n = 21$). ChABC or control solution was delivered on alternate days for 10 days after lesion. Control animals received sham surgery ($n = 20$). Rats were perfused at 2 weeks after lesion to check effectiveness of treatment in removing CS-GAG ($n = 4$ per group), tested behaviourally over 6 weeks ($n = 5$, 9 and 8 for ChABC, vehicle and sham, respectively), then perfused at 8 weeks after lesion for anatomical analysis of ascending systems ($n = 4$ per group), perfused at 10 weeks after lesion for analysis of CST regeneration ($n = 4$ per group), or used for terminal electrophysiology experiments at 13–17 days after lesion ($n = 4$ per group).

Confirmation of CS-GAG digestion

Tissue processing was as described previously[29]. Parasagittal sections (20 μm) of cervical spinal cord were immunostained using monoclonal antibody 2B6 (Seikagaku Corporation, 1:5,000), with tyramide signal amplification (NEN). Some tissue sections from lesioned cords treated with vehicle *in vivo* were incubated *in vitro* with ChABC (0.2 U ml^{-1}, 2 h, 37 °C). We processed tissue from all experimental conditions in parallel.

GAP-43 analysis in DRG neurons

Sections of C5 and C6 DRG (10 μm) were double-immunostained for βIII tubulin (Promega, 1:1000) to identify all neurons, and for the growth-associated protein GAP-43 (gift from G. Wilkin, 1:2000), using 7-amino-4-methylcoumarin-3-acetic-acid- and tetramethylrhodamine isothiocyanate (TRITC)-conjugated secondary antibodies. The percentage of GAP-43-positive cells was determined in four sections per animal.

Axon tract tracing in the spinal cord

Ascending dorsal column axons were labelled using the CTB tracer[29], injected into the left median nerve of anaesthetized rats. Longitudinal sections (20 μm) were immunostained for glial fibrillary acidic protein, to identify the lesion site, and for CTB, to identify the labelled dorsal column axons[29]. Descending CST axons were labelled with 1 μl BDA (Molecular Probes; 10% in saline) injected under anaesthesia at four sites over the left primary motor cortex, 1 mm below the dorsal surface of the brain. BDA-labelled fibres were visualized in parasaggittal spinal cord sections (20 μm) with extra-avidin conjugated to fluorescein isothiocyanate. All BDA-labelled fibres observed within a 1-mm square grid were counted at measured intervals from 4 mm above to 5 mm below the lesion site by an experimenter, blinded to treatment. Due to variability in labelling, axon numbers were calculated as a percentage of the fibres seen 4 mm above the lesion, where the CST was intact. To confirm a complete CST lesion, transverse lumbar spinal cord sections (20 μm) were immunostained with an antibody against the γ-subunit of protein kinase C (PKC-γ, Santa Cruz, 1:1000), visualized with a TRITC-conjugated secondary antibody.

Electrophysiology

In terminal electrophysiological experiments, the sensory motor cortex and cervical spinal cord were exposed in urethane-anaesthetized (1.5 g kg^{-1}) rats. Cortical evoked potentials were elicited by electrical stimulation (five square-wave pulses at 400 Hz, 100 μA, 200 μs, delivered every 2 s) of the left sensory motor cortex using a 0.5-mm concentric needle electrode lowered 1 mm into the cortex. For each experiment we mapped the optimal stimulation site, located 1–2 mm lateral and 1 mm rostrocaudal from Bregma. Postsynaptic potentials evoked by the cortical stimuli were recorded with a silver ball electrode placed medially on the contralateral cord surface. At each recording site (1 segment above and 1–7 mm below the lesion at C4), 64 responses were averaged and stored for off-line analysis of response magnitude (area under curve) and latency.

Behavioural assessment

After baseline testing, we tested animals once a week for 6 weeks after lesion. We averaged right and left forepaw scores, as no differences were observed between them. Experimenters were blind to the treatment. A tape removal test (adapted from ref. 24) produced separate scores for sensory and motor behaviour. Adhesive tape (0.3 inch × 1 inch) was placed on the forepaw, and the time taken to sense the presence of the tape (indicated by paw shake) was determined. For animals that sensed the tape, the removal time was also scored. Rats were tested on two locomotor tasks requiring sensorimotor integration (adapted from ref. 30). Rats were trained to cross a narrow metal beam (1.25 inch × 36 inches) and a wire grid (12 inches × 36 inches with 1 inch × 1 inch grid squares). Forepaw foot slips were recorded (determined by a paw slipping off the beam or below the plane of the grid). In a footprint analysis (adapted from ref. 30), rat forepaws were covered with ink to record walking patterns during continuous locomotion across a wooden runway (4 inches × 36 inches), and stride length and width were calculated.

Received 4 September 2001; accepted 8 February 2002.

1. Fawcett, J. W. & Asher, R. A. The glial scar and central nervous system repair. *Brain Res. Bull.* **49,** 377–391 (1999).
2. Fitch, M. T. & Silver, J. *CNS Regeneration: Basic Science and Clinical Advances* (eds Tuszynski, M. H. & Kordower, J. H.) 55–88 (Academic, San Diego, 1999).
3. McKeon, R. J., Schreiber, R. C., Rudge, J. S. & Silver, J. Reduction of neurite outgrowth in a model of glial scarring following CNS injury is correlated with the expression of inhibitory molecules on reactive astrocytes. *J. Neurosci.* **11,** 3398–3411 (1991).
4. Smith-Thomas, L. C. *et al.* An inhibitor of neurite outgrowth produced by astrocytes. *J. Cell Sci.* **107,** 1687–1695 (1994).
5. Niederost, B. P., Zimmermann, D. R., Schwab, M. E. & Bandtlow, C. E. Bovine CNS myelin contains neurite growth-inhibitory activity associated with chondroitin sulfate proteoglycans. *J. Neurosci.* **19,** 8979–8989 (1999).
6. Davies, S. J., Goucher, D. R., Doller, C. & Silver, J. Robust regeneration of adult sensory axons in degenerating white matter of the adult rat spinal cord. *J. Neurosci.* **19,** 5810–5822 (1999).
7. McKeon, R. J., Hoke, A. & Silver, J. Injury-induced proteoglycans inhibit the potential for laminin-mediated axon growth on astrocytic scars. *Exp. Neurol.* **136,** 32–43 (1995).
8. Zuo, J., Neubauer, D., Dyess, K., Ferguson, T. A. & Muir, D. Degradation of chondroitin sulfate proteoglycan enhances the neurite-promoting potential of spinal cord tissue. *Exp. Neurol.* **154,** 654–662 (1998).
9. Fidler, P. S. *et al.* Comparing astrocytic cell lines that are inhibitory or permissive for axon growth: the major axon-inhibitory proteoglycan is NG2. *J. Neurosci.* **19,** 8778–8788 (1999).
10. Moon, L. D., Asher, R. A., Rhodes, K. E. & Fawcett, J. W. Regeneration of CNS axons back to their target following treatment of adult rat brain with chondroitinase ABC. *Nature Neurosci.* **4,** 465–466 (2001).
11. Chong, M. S. *et al.* GAP-43 expression in primary sensory neurons following central axotomy. *J. Neurosci.* **14,** 4375–4384 (1994).
12. Bradbury, E. J., McMahon, S. B. & Ramer, M. S. Keeping in touch: sensory neurone regeneration in the CNS. *Trends Pharmacol. Sci.* **21,** 389–394 (2000).
13. Mori, M., Kose, A., Tsujino, T. & Tanaka, C. Immunocytochemical localization of protein kinase C subspecies in the rat spinal cord: light and electron microscopic study. *J. Comp Neurol.* **299,** 167–177 (1990).
14. Hill, C. E., Beattie, M. S. & Bresnahan, J. C. Degeneration and sprouting of identified descending supraspinal axons after contusive spinal cord injury in the rat. *Exp. Neurol.* **171,** 153–169 (2001).
15. Wall, P. D. & Lidierth, M. Five sources of a dorsal root potential: their interactions and origins in the superficial dorsal horn. *J. Neurophysiol.* **78,** 860–871 (1997).
16. Ramer, M. S., Priestley, J. V. & McMahon, S. B. Functional regeneration of sensory axons into the adult spinal cord. *Nature* **403,** 312–316 (2000).
17. Murray, M. Strategies and mechanisms of recovery after spinal cord injury. *Adv. Neurol.* **72,** 219–225 (1997).
18. Levine, J. M. Increased expression of the NG2 chondroitin-sulfate proteoglycan after brain injury. *J. Neurosci.* **14,** 4716–4730 (1994).
19. McKeon, R. J., Jurynec, M. J. & Buck, C. R. The chondroitin sulfate proteoglycans neurocan and phosphacan are expressed by reactive astrocytes in the chronic CNS glial scar. *J. Neurosci.* **19,** 10778–10788 (1999).
20. Asher, R. A. *et al.* Neurocan is upregulated in injured brain and in cytokine-treated astrocytes. *J. Neurosci.* **20,** 2427–2438 (2000).
21. Plant, G. W., Bates, M. L. & Bunge, M. B. Inhibitory proteoglycan immunoreactivity is higher at the caudal than the rostral Schwann cell graft-transected spinal cord interface. *Mol. Cell Neurosci.* **17,** 471–487 (2001).
22. Bregman, B. S. *et al.* Recovery from spinal cord injury mediated by antibodies to neurite growth inhibitors. *Nature* **378,** 498–501 (1995).
23. Pasterkamp, R. J., Anderson, P. N. & Verhaagen, J. Peripheral nerve injury fails to induce growth of lesioned ascending dorsal column axons into spinal cord scar tissue expressing the axon repellent Semaphorin3A. *Eur. J. Neurosci.* **13,** 457–471 (2001).
24. Thallmair, M. *et al.* Neurite growth inhibitors restrict plasticity and functional recovery following corticospinal tract lesions. *Nature Neurosci.* **1,** 124–131 (1998).
25. Ramer, M. S., Harper, G. P. & Bradbury, E. J. Progress in spinal cord research—a refined strategy for the International Spinal Research Trust. *Spinal Cord* **38,** 449–472 (2000).
26. Fouad, K., Dietz, V. & Schwab, M. E. Improving axonal growth and functional recovery after experimental spinal cord injury by neutralizing myelin associated inhibitors. *Brain Res. Brain Res. Rev.* **36,** 204–212 (2001).
27. Jones, L. L., Oudega, M., Bunge, M. B. & Tuszynski, M. H. Neurotrophic factors, cellular bridges and gene therapy for spinal cord injury. *J. Physiol.* **533,** 83–89 (2001).
28. Murray, M. & Fischer, I. Transplantation and gene therapy: combined approaches for repair of spinal cord injury. *Neuroscientist* **7,** 28–41 (2001).
29. Bradbury, E. J. *et al.* NT-3 promotes growth of lesioned adult rat sensory axons ascending in the dorsal columns of the spinal cord. *Eur. J. Neurosci.* **11,** 3873–3883 (1999).
30. Kunkel-Bagden, E., Dai, H. N. & Bregman, B. S. Methods to assess the development and recovery of locomotor function after spinal cord injury in rats. *Exp. Neurol.* **119,** 153–164 (1993).

Acknowledgements

We thank T. J. Boucher for critical review of the manuscript and J. V. Priestley, M. Lidierth, B. J. Kerr and M. S. Ramer for their help. This work was supported by The Wellcome Trust, MRC, International Spinal Research Trust and Action Research.

Competing interests statement

The authors declare that they have no competing financial interests.

Correspondence and requests for materials should be addressed to E.J.B. (e-mail: elizabeth.bradbury@kcl.ac.uk).

The *Drosophila* immune response against Gram-negative bacteria is mediated by a peptidoglycan recognition protein

Marie Gottar*, Vanessa Gobert*, Tatiana Michel*, Marcia Belvin†, Geoffrey Duyk†, Jules A. Hoffmann*, Dominique Ferrandon*‡ & Julien Royet*‡

** UPR 9022 du Centre National de la Recherche Scientifique, Institut de Biologie Moléculaire et Cellulaire, 15 rue René Descartes, F67084 Strasbourg, Cedex, France*
† Exelixis Inc., South San Francisco, California 94083, USA
‡ These authors contributed equally to this work

The antimicrobial defence of *Drosophila* relies largely on the challenge-induced synthesis of an array of potent antimicrobial peptides by the fat body[1,2]. The defence against Gram-positive bacteria and natural fungal infections is mediated by the Toll signalling pathway, whereas defence against Gram-negative bac-